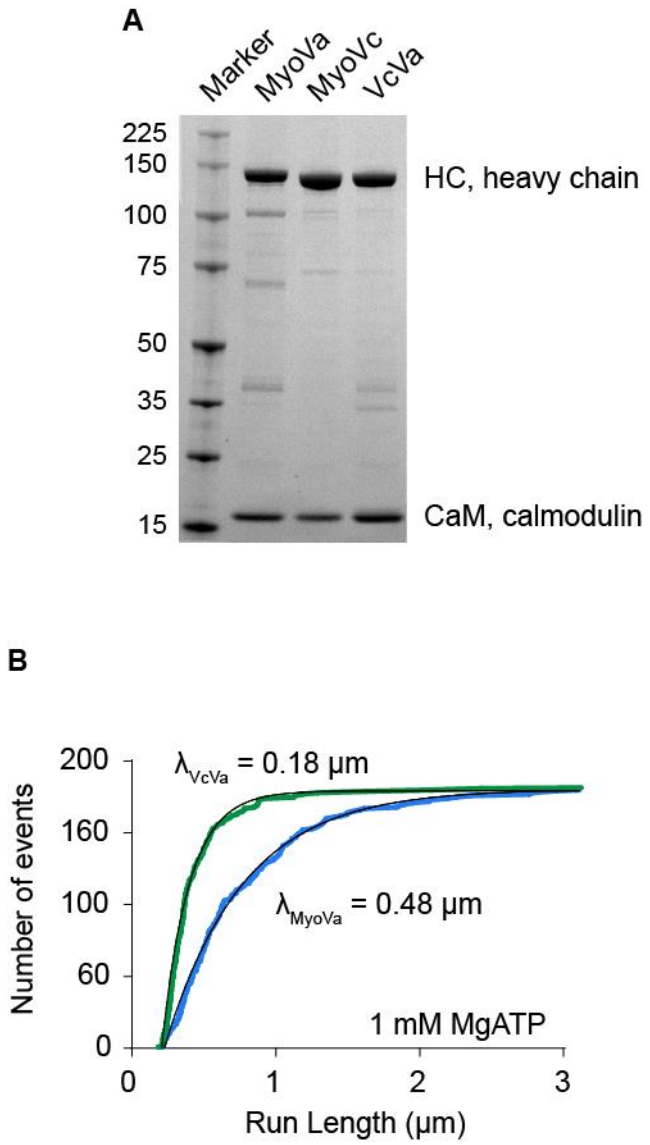

Figure S1. SDS-PAGE gel of myosin constructs and run length distributions for VcVa and MyoVa on single actin filaments. Related to Figure 1.

SDS-PAGE gel of myosin constructs and run length distributions for VcVa and MyoVa on single actin filaments. (A) SDS-PAGE gel (4-12% gradient with MOPS running buffer) of the affinity purified baculovirus/Sf9 expressed myosin constructs. (B) Cumulative frequency distribution of run lengths comparing MyoVa (blue) and the VcVa chimera (green) at 1mM MgATP. Run lengths, λ, were determined from an exponential fit (black line).

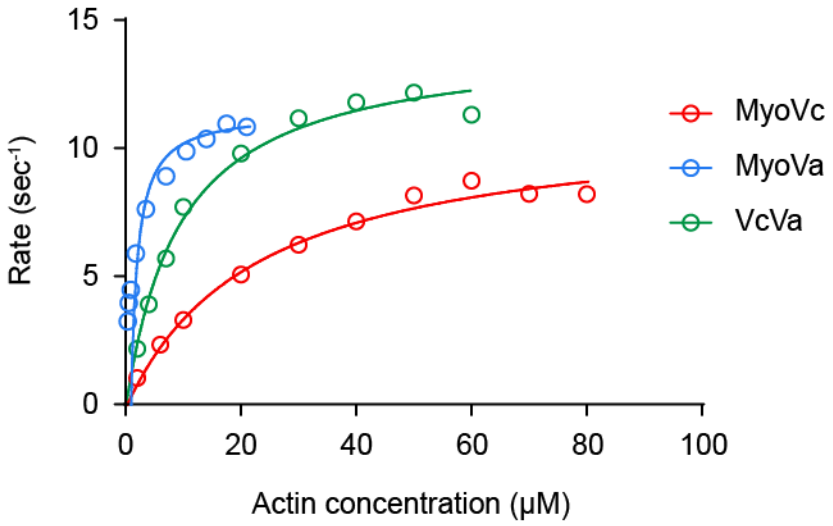

Figure S2. Actin-activated ATPase for MyoVc, MyoVa and VcVa-HMM constructs. Related to Figure 1.
A linked ATPase assay was used to determine the steady state actin activated ATPase activity at 30ºC for MyoVc (red), MyoVa (blue) and VcVa chimera (green); MyoVc, V_{max} = 11.23 sec^{-1} ± 0.56, K_m = 22.93 ± 3.24; MyoVa, V_{max} = 10.91 sec^{-1} ± 0.36, K_m = 1.29 ± 0.19; VcVa, V_{max} = 14.19 sec^{-1} ± 0.51, K_m = 9.49 ± 1.15. The basal ATPase rate in the absence of actin is reported between 0.05-0.1 sec^{-1} [S1, S2]. ATPase assays were performed in buffers containing 10 mM Imidazole, pH 7.4, 1 mM $MgCl_2$, 1 mM EGTA, 1 mM dithiothreitol and 25 mM NaCl.

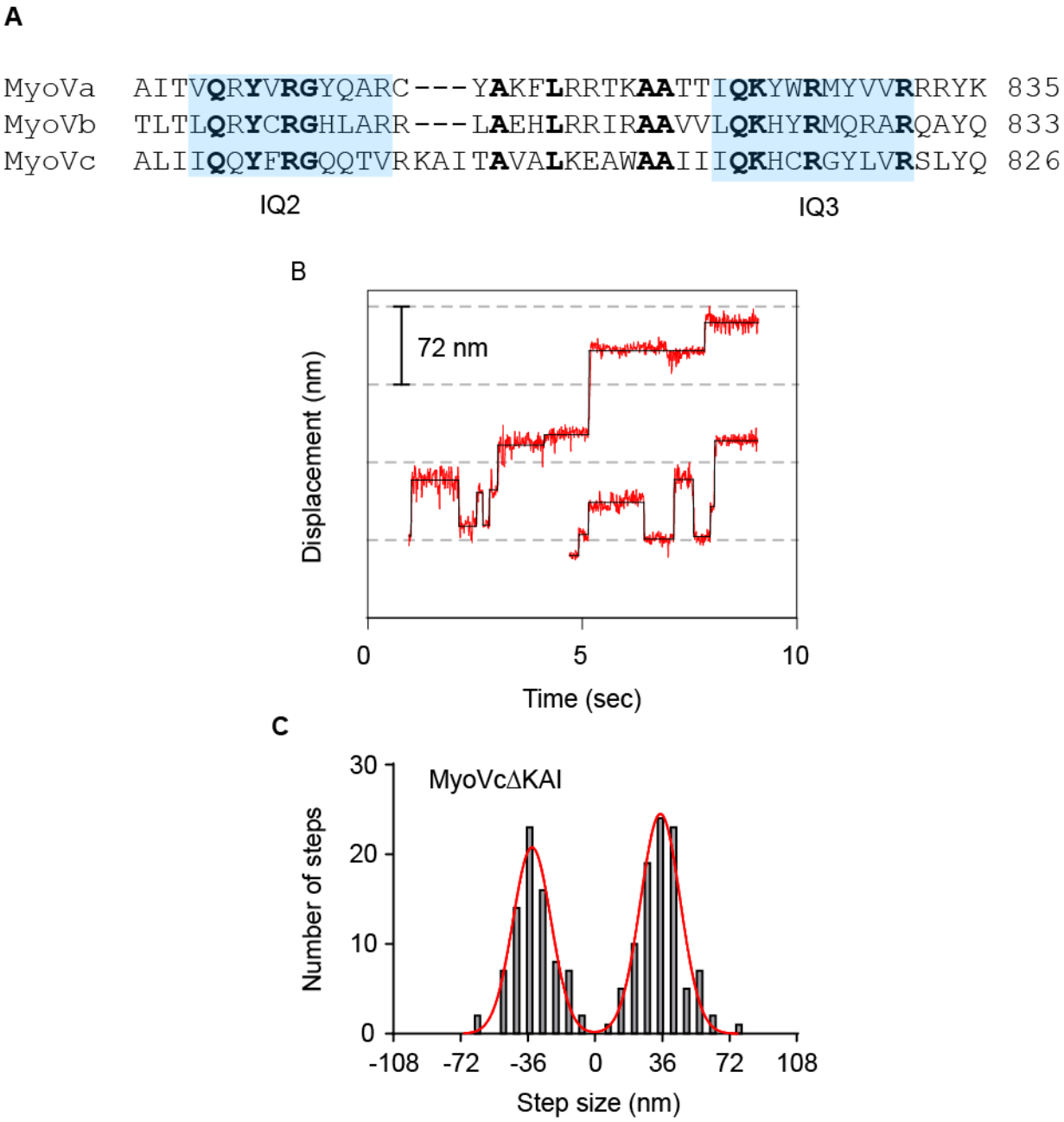

Figure S3. Structural comparisons of human class V myosins, the step size distribution of MyoVcΔKAI and MyoVc stepping with a Qdot bound to the motor domain on single actin filaments. Related to Figure 1.

(A) Partial alignment of the second and third calmodulin-binding IQ motifs in the lever arm of the three mammalian class V myosins, MyoVa, MyoVb and MyoVc. IQ motifs are in blue. A unique 3 amino acid insert (KAI) following IQ motif 2 in MyoVc increases the spacing between these two motifs in class V myosins.
(B) Stepping dynamics on single actin filaments of MyoVc containing a biotin tag on the N-terminus for Qdot attachment.
(C) Step size distribution of MyoVcΔKAI. Step size histogram of a MyoVc construct where the 3-amino insert (KAI) between IQ motifs 2 and 3 has been deleted (MyoVcΔKAI). The step size histogram was fit to multiple Gaussian distributions to determine the average step sizes ± SD for MyoVcΔKAI; 35.0 nm ± 10.2 and -33.7 nm ± 10.6 (N = 176).

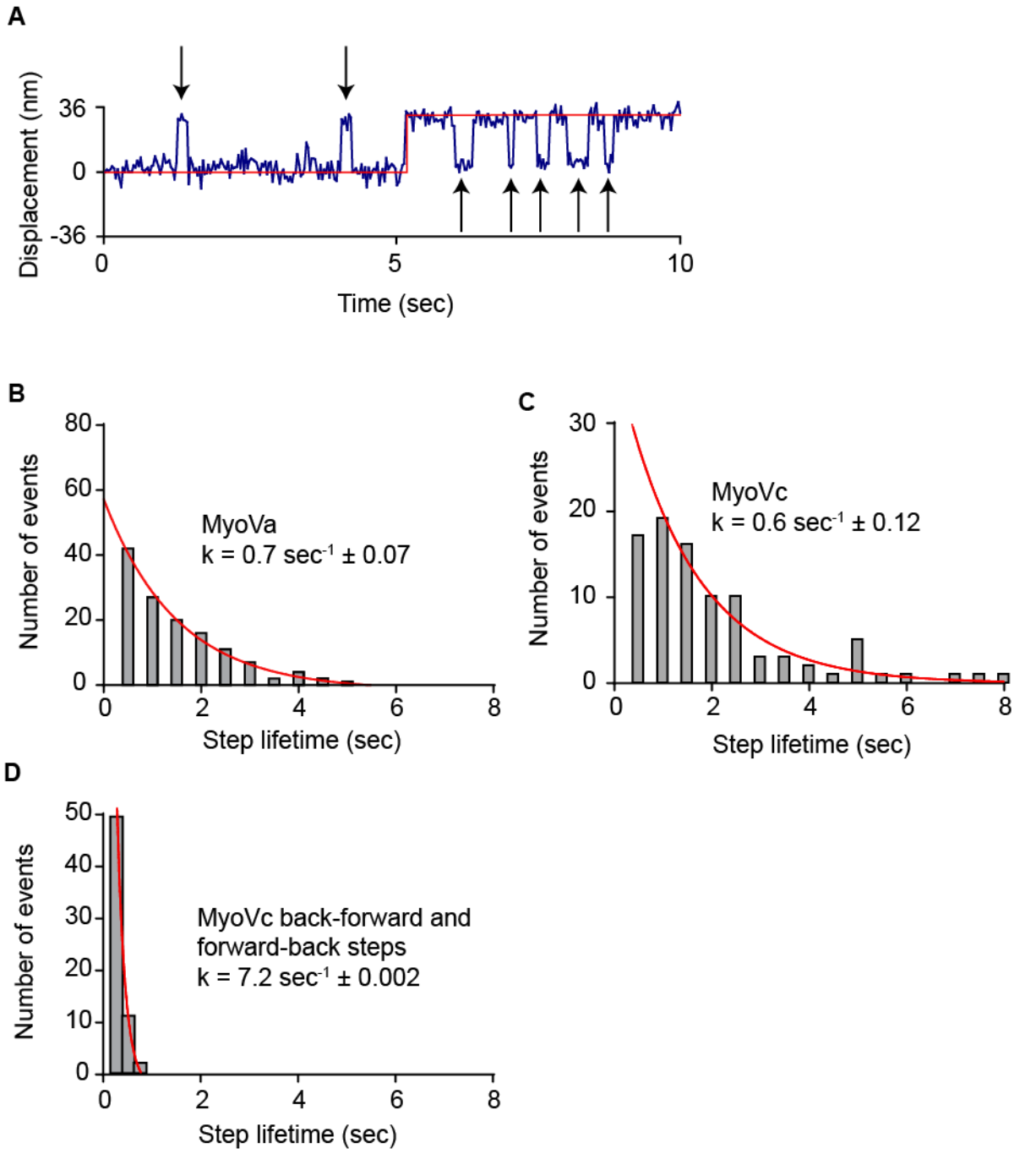

Figure S4. MyoVc shows distinct back-forward and forward-back steps with short step lifetimes. Related to Figure 1.

(A) Time and displacement plot of a single MyoVc motor stepping on an actin filament. The plot is a cropped stepping trace showing one step (red line) and 7 back-forward and forward-back steps with short lifetimes (arrows). **(B–D)** Step lifetime histograms of **(B)** MyoVa, **(C)** MyoVc with forward-back and back-forward events removed, and **(D)** MyoVc forward-back and back-forward events defined as having a dwell time less than 0.6 sec at 0.5μM MgATP. The lifetime distributions were fitted to Y = A*exp(-X/t) where the stepping lifetime (k) = 1/t. For (C), the first bin was not included in the fitting.

Supplemental Experimental Procedures

Protein constructs

cDNA encoding full-length human MyoVc was kindly provided by Dr. Richard Cheney (University of North Carolina at Chapel Hill). Sequences of the heavy meromyosin subfragment (HMM) of MyoVc (amino acids 1-1105) and mouse MyoVa (amino acids 1-1098) were sub-cloned into pAcSG2. All myosin constructs contained a C-terminal biotin tag for attachment to streptavidin conjugated–Qdots with the exception of the N-terminally biotin tagged MyoVc construct for N-terminal Qdot attachment used for stepping (Invitrogen) [S3]. Biotin tags were followed by an 8-amino acid Flag tag for purification by affinity chromatography. The VcVa chimeric construct was made by replacing the lever arm and rod sequences of MyoVc (amino acids K750-E1105) with those of MyoVa (amino acids K760-E1098). The VaVc chimera was made by replacing the motor domain sequences of MyoVc (amino acids M1-K750) with those of MyoVa (amino acids M1-K760). Constructs were verified by DNA sequencing. Calcium insensitive CaM (CaMΔall) was co-expressed with myoVa as described previously [S4]. A pET11d vector containing rat Tpm1.8 (previously Tm5a) was a generous gift from Dr. Sarah Hitchcock-DeGregori (Rutgers Robert Wood Johnson Medical School). Human Tpm3.1 (previously Tm5nm1) and Tpm4.2 (previously Tm4) in pET3a were kindly provided by Dr. Matthew Lord (University of Vermont). These constructs included an alanine and serine before the start codon to mimic acetylation [S5]. The construct used for fascin expression is described previously [S6].

Protein expression and purification

Myosin heavy chain constructs were co-expressed with calmodulin that lacks functional calcium binding sites (CaMΔall) [S4], using the baculovirus/ Sf9 insect cell expression system. Expressed myosin was purified by Flag-affinity chromatography as described previously [S7] except that MyoVc preparations were washed in the presence of 50 μM MgATP and eluted with buffer containing 25 μg/ml CaMΔall to reduce aggregation due to possible dissociation of CaMΔall from the lever arm, and 50 μM MgATP. Preparations were stored at -20ºC in storage buffer (25 mM imidazole, pH 7.4, 300 mM KCl, 1 mM EGTA, 4 mM $MgCl_2$ and 1 mM DTT) containing 50 μM MgATP and 0.1 mg/ml CaMΔall. Purification of bacterially expressed CaMΔall is described previously [S4]. Human fascin was expressed in BL21(DE3) cells and purified [S6]. Tropomyosin was purified according to Hodges et al [S8]. Chicken skeletal actin was purified from acetone powder [S9].

Fluorescent labeling of actin

Globular actin (G-actin) was diluted to 1 mg/ml with G buffer (5 mM Tris-HCl, pH 8.0, 0.2 mM $CaCl_2$, 0.2 mM DTT and 0.2 mM NaATP), clarified at 350,000g for 25 min and protein concentration after clarification was determined by a Bradford assay. G-actin was polymerized by addition of 10 μl of 10x polymerization buffer (500 mM KCl, 20 mM $MgCl_2$ and 1 mM MgATP) to 90 μl actin and incubated for 60 min at room temperature. To label polymerized actin (F- actin), 0.54 nmols of dried tetramethylrhodamine isothiocyanate (TRITC) phalloidin or Alexa Fluor635 phalloidin (Invitrogen) was re-suspended with 5 μl of 100% methanol. To this, 500 μl of motility buffer (25 mM imidazole, pH 7.4, 25 mM KCl, 1 mM EGTA, 4 mM $MgCl_2$ and 1 mM DTT) containing 0.8 μM F-actin and 2 μM Tpm3.1 was added.

Actin bundles were made similarly except motility buffer containing freshly polymerized 0.8 μM F actin, 2 μM Tpm3.1, and 1.2 μM fascin was added to TRITC-phalloidin and incubated at 4ºC for ~3 days.

Total internal reflection fluorescence (TIRF) microscopy

Myosin was diluted to 0.8 mg/ml in buffer A (25 mM imidazole, pH 7.4, 300 mM KCl, 1 mM EGTA, 4 mM $MgCl_2$ and 1 mM DTT) containing 0.2 mg/ml CaMΔall, 0.3 mg/ml F-actin, and 2 mM MgATP. This mixture was immediately spun at 350,000g for 15 min and protein concentration of the supernatant was determined by a Bradford assay. Concentration of the myosin heavy chain was corrected for added CaMΔall. The concentration of the heavy chain was further verified using gel densitometry against a known concentration standard. For single motor processivity experiments, 0.02–0.04 μM myosin dimers were mixed with 0.2 μM Qdots in buffer A. This results in a 5–10-fold molar excess of Qdots over myosin dimers which ensures that the majority of motile Qdots are bound to a single motor. For multiple motor ensemble experiments, 0.5 μM myosin dimers were mixed with 0.05 μM Qdots in buffer A, resulting in a 10-fold molar excess of myosin and the recruitment of multiple motors per Qdot.

Flow cells containing labeled actin bound to Tpm3.1 were prepared as described previously [S3]. For imaging the motility of a single motor bound to a Qdot at high MgATP concentrations, myosin–Qdot mixtures (5-10 Qdots per 1 myosin dimer) were diluted to 0.5–1.0 nM (myosin dimer concentration) in buffer B (25 mM imidazole,

pH 7.4, 25 mM KCl, 1 mM EGTA, 4 mM $MgCl_2$, 1 mM DTT, and ATP-regeneration and oxygen-scavenging systems [S3]) containing 0.2 mg/ml CaMΔall, 2 μM Tpm3.1, and 1 mM MgATP. Single motor experiments that were supplemented with MgADP contained no MgATP-regeneration system. For comparing single motor motility on actin bundles and single actin filaments, myosin–Qdot dilutions from the same mixture were added to a split flow cell bound to actin filaments on one side and actin bundles on the other. For single motor stepping data, myosin–Qdot mixtures (5-10 Qdots per 1 myosin dimer) were diluted to 0.1 nM for MyoVc and 0.03 nM for MyoVa in buffer B containing 0.2 mg/ml CaMΔall, 2 μM Tpm3.1, and 0.5 μM MgATP and added to a flow cell bound to labeled actin filaments or actin bundles.

For visualizing multiple motors bound to a Qdot, myosin–Qdot mixtures (1 Qdot per 10 myosin dimers) were diluted 1/100 in buffer B containing 0.2 mg/ml CaMΔall, 2 μM Tpm3.1, and 1 mM MgATP for a final Qdot concentration of 0.5 nM and added to a flow cell containing labeled actin filaments or actin bundles.

Data were collected using through-the-objective TIRF microscopy built on an inverted microscope (Eclipse Ti-U; Nikon) equipped with a 1003 Plan Apo objective lens (1.49 NA), air table and 1.5X auxiliary magnification. Qdot 655 (Invitrogen) and Alexa Fluor 488 (Invitrogen) was excited with a 473-nm argon laser. Images were captured using an XR/Turbo-Z camera (Stanford Photonics) controlled with Piper software (v2.3.39) typically at 30 frames per second with a 4-frame integration period. The pixel size was determined to be 93 nm. To obtain run length and speed data at 1 mM MgATP, Qdots and beads were tracked with ImageJ (National Institute of Health) using the sub-pixel particle tracking plug-in MTrackJ [S10]. Run trajectories were made by tracking Qdots with the ImageJ plug-in, SpotTracker and plotting the x,y positions of the Qdot.

Stepping of single myosin motors bound to a Qdot on single actin filaments was resolved at 0.5 μM MgATP. Qdots were tracked using the ImageJ plug-in, SpotTracker and verified using a custom MATLAB program that fits the point spread function of the Qdot to a two-dimensional Gaussian distribution [S11]. To determine step sizes, x,y coordinates were used to calculate displacement versus time. Step sizes were fit to this data using a Kerssemakers step-finding algorithm written in MATLAB [S12].

Actin-activated ATPase assays

Linked actin-activated ATPase assays were performed at 30°C in 10 mM imidazole, pH 7.4, 25 mM KCl, 1 mM $MgCl_2$, 1 mM EGTA, 1 mM DTT, 1 mM MgATP and 0.1 mg/ml CaMΔall. Buffers also included an ATP regeneration system (0.2 mM NADH, 0.5 mM phosphoenolpyruvate, 20 U/ml lactate dehydrogenase, and 100 U/ml pyruvate kinase) to minimize ADP-inhibition of the motor. The rate was determined by measuring the oxidation of NADH by lactate dehydrogenase at 340 nm [S13].

Stepping analysis on actin bundles

The positions of Qdots bound to a single myosin motor were tracked at 30 frames per second moving on actin bundles at 0.5 μM MgATP using the ImageJ plug-in, SpotTracker. The axis of the actin bundle relative to each run trajectory was determined using the ImageJ plug-in NeuronJ [S14, S15]. x,y data was rotated in Excel such that the center of the bundle establishes the position of the x-axis in a coordinate system. To identify the position of each step, x,y data over a 1000-frame movie were classified into ~8-20 positions along the bundle per run. x.y data was averaged at each position to identify the center of the actin binding site. Eight representative run trajectories were analyzed per condition giving over 200 steps. Angles between successive steps were calculated in Excel as described previously [S16]. The average lateral displacement per step was calculated by measuring distance along the y-axis between each step.

Supplemental References

S1. Watanabe, S., Watanabe, T.M., Sato, O., Awata, J., Homma, K., Umeki, N., Higuchi, H., Ikebe, R., and Ikebe, M. (2008). Human myosin Vc is a low duty ratio nonprocessive motor. J Biol Chem *283*, 10581-10592.

S2. Takagi, Y., Yang, Y., Fujiwara, I., Jacobs, D., Cheney, R.E., Sellers, J.R., and Kovacs, M. (2008). Human myosin Vc is a low duty ratio, nonprocessive molecular motor. J Biol Chem *283*, 8527-8537.

S3. Krementsova, E.B., Hodges, A.R., Bookwalter, C.S., Sladewski, T.E., Travaglia, M., Sweeney, H.L., and Trybus, K.M. (2011). Two single-headed myosin V motors bound to a tetrameric adapter protein form a processive complex. J Cell Biol *195*, 631-641.

S4. Krementsov, D.N., Krementsova, E.B., and Trybus, K.M. (2004). Myosin V: regulation by calcium, calmodulin, and the tail domain. J Cell Biol *164*, 877-886.

S5. Maytum, R., Geeves, M.A., and Konrad, M. (2000). Actomyosin regulatory properties of yeast tropomyosin are dependent upon N-terminal modification. Biochemistry *39*, 11913-11920.

S6. Hodges, A.R., Bookwalter, C.S., Krementsova, E.B., and Trybus, K.M. (2009). A nonprocessive class V myosin drives cargo processively when a kinesin- related protein is a passenger. Curr Biol *19*, 2121-2125.

S7. Krementsova, E.B., Hodges, A.R., Lu, H., and Trybus, K.M. (2006). Processivity of chimeric class V myosins. J Biol Chem *281*, 6079-6086.

S8. Hodges, A.R., Krementsova, E.B., Bookwalter, C.S., Fagnant, P.M., Sladewski, T.E., and Trybus, K.M. (2012). Tropomyosin is essential for processive movement of a class v Myosin from budding yeast. Curr Biol *22*, 1410-1416.

S9. Pardee, J.D., and Spudich, J.A. (1982). Purification of muscle actin. Methods Enzymol *85 Pt B*, 164-181.

S10. Meijering, E., Dzyubachyk, O., and Smal, I. (2012). Methods for cell and particle tracking. Methods Enzymol *504*, 183-200.

S11. Ali, M.Y., Lu, H., Bookwalter, C.S., Warshaw, D.M., and Trybus, K.M. (2008). Myosin V and Kinesin act as tethers to enhance each others' processivity. Proc Natl Acad Sci U S A *105*, 4691-4696.

S12. Kerssemakers, J.W., Munteanu, E.L., Laan, L., Noetzel, T.L., Janson, M.E., and Dogterom, M. (2006). Assembly dynamics of microtubules at molecular resolution. Nature *442*, 709-712.

S13. De La Cruz, E.M., Wells, A.L., Sweeney, H.L., and Ostap, E.M. (2000). Actin and light chain isoform dependence of myosin V kinetics. Biochemistry *39*, 14196-14202.

S14. Meijering, E., Jacob, M., Sarria, J.C., Steiner, P., Hirling, H., and Unser, M. (2004). Design and validation of a tool for neurite tracing and analysis in fluorescence microscopy images. Cytometry A *58*, 167-176.

S15. Ricca, B.L., and Rock, R.S. (2010). The stepping pattern of myosin X is adapted for processive motility on bundled actin. Biophys J *99*, 1818-1826.

S16. Yusuf Ali, M., Previs, S.B., Trybus, K.M., Sweeney, H.L., and Warshaw, D.M. (2013). Myosin VI has a One Track Mind Versus Myosin Va When Moving on Actin Bundles or at an Intersection. Traffic *14*, 70-81.